MATHEMATICAL MODELING AND COMPUTING, Vol. 8, No. 4, pp. 678–690 (2021)

Optimal variable support size for mesh-free approaches using genetic algorithm

Hassouna S., Timesli A.

Hassan II University of Casablanca,
National Higher School of Arts and Crafts (ENSAM Casablanca),
20670 Casablanca, Morocco

(Received 23 May 2021; Accepted 7 June 2021)

The main difficulty of the meshless methods is related to the support of shape functions. These methods become stable when sufficiently large support is used. Rather larger support size leads to higher calculation costs and greatly degraded quality. The continuous adjustment of the support size to approximate the shape functions during the simulation can avoid this problem, but the choice of the support size relative to the local density is not a trivial problem. In the present work, we deal with finding a reasonable size of influence domain by using a genetic algorithm coupled with high order mesh-free algorithms which the optimal value depends on the accuracy and stability of the results. The proposed strategy provides guarantees about the growth of approximation errors, monitor the level of error, and adapt the evaluation strategy to reach the required level of accuracy. This allows the adaptation of the proposed algorithm with problem complexity. This new strategy in meshless approaches are tested on some examples of structural analysis.

Keywords: *large deformations, strong form, meshless method, genetic algorithm, automatic choice of nearest neighbors.*

2010 MSC: 65D05, 65M99, 74D10, 41A58, 74M15 **DOI:** 10.23939/mmc2021.04.678

1. Introduction

In our opinion, the main advantage of meshless methods in nonlinear structural analysis is the possibility to handle more flexibly large transformations and discontinuities than the Finite Element Method (FEM) approaches that typically suffer from severe grid distortion under these conditions. Meshless methods are used to study elastoplasticity and hyperelasticity problems [1–6], viscoplastic problems [7–10], fissuring of structures [11–13], contact problems [14], nonlinear dynamic ruptures [15], metal forming problems [16] and there are other fields of application of meshless methods. The performance of meshless methods can be explained by the following factors: (i) in the Lagrangian formulation, the gradient operator of the transformation calculated at a point is constructed using a number of nearest neighbors generally larger than the only nodes of the element in the FEM; (ii) in meshless approaches based on the strong form there is no Jacobian matrix, even in the case of meshless approaches based on the weak form, the Jacobian matrix associated not become singular except for much larger distortion of nearest neighbors [17]; (iii) the quality of the solution is much less sensitive to the relative position of the nodes, authorizing in updated Lagrangian formulations to build the solution from relative positions between the nodes prohibited in the finite element method; (iv) it is not necessary to build a mesh for the construction of approximations that allows treating the domains of complex geometries in bidimensional ($2D$) or tridimensional ($3D$) cases, using only a cloud of nodes [18]; (v) another major advantage of meshless methods is the ability to insert or remove nodes very easily, the relative position of the nodes between them influences very little the solution quality. There are other advantages of the meshless methods which are related to the physical phenomenon to simulate, for example, the meshfree shape functions reduce considerably the dependence between the direction of the shear bands or cracks and nodes distribution [19, 20]. The conditions necessary to

guarantee the stability of these methods are given in [21–23]. The use of fixed support in the problems simulation where the cloud of nodes undergoes strong distortions can involve the instability of the method. Relatively large support of the Moving Least Square (MLS) shape functions allows remedying for the blocking problems encountered in the incompressibility problems. Li et al. [17] conduct a large deformation simulation with a displacement formulation without introducing a specific treatment for the problems related to plastic incompressibility. In the same way in [17], the volumetric locking and shear locking problems encountered in the FEM are not encountered with the meshless methods. When we want to reduce the support size, for reasons of cost and quality, the blocking problems reappear. These aspects are discussed in [24, 25]. We can notice that the main difficulty of these techniques is related to the support of the shape functions. In most of these approaches, the support domain (or also influence domain) of a node is defined by a sphere or a parallelepiped centered on this node and by a circle or rectangle in the $3D$ and $2D$ cases respectively. As discussed by Liu et al. [22, 23, 26], this support must cover a sufficient number of nodes (or particles), so it must be large enough, so that the method to be stable. Rather, a larger support size leads to greatly degraded quality and higher calculation costs. To avoid these problems, we can use the continuous adjustment of the support size of the shapes functions during the simulation, but the search for optimal support size relative to the local density is not a trivial problem. In the proposed meshless approaches [6, 8–10, 27, 28], the nearest neighbors (N) choice can be determined from numerical tests to stabilize the solution which is very difficult and expensive in terms of calculation time.

Timesli [29] presented the first effort to find the optimal size of the influence domain for high order mesh-free algorithms. In this paper, we propose an adaptive approach to optimize the support size of meshfree shape functions. Our objective is to show a mesh-free approach coupled with a genetic algorithm to determines, with good precision, the optimal value of the support size. It is an effective strategy coupling the high order mesh-free approach, based on strong form MLS approximations, and an optimal value search algorithm of the support size based on optimization algorithms to ensure the existence of the inversion of weighted moment matrix $[A]^{-1}$ and a well-conditioned $[A]$ in MLS approximation. In this approach, the choice of nearest neighbors depends on the accuracy and stability of the results.

The outline of this paper is as follows: Section 2 presents the high order approaches of the considered nonlinear problem. In Section 3, the promising genetic algorithm for finding a good size of influence domain for solving large deformation problems by the high order mesh-free approaches is introduced. The results of numerical experiments are presented in Section 4. Finally, we finish with a conclusion in section 5.

2. High order approaches of the considered nonlinear problem

In the nonlinear elastic contact problems with large deformations, the problem in strong form as shown in the reference [6] can be written as follows:

$$\begin{cases} \operatorname{div} \boldsymbol{T} = 0 & \text{on} \quad \Omega, \\ T = S + BS, & \\ S = D : \gamma, & \\ T \cdot N_F = \lambda F & \text{on} \quad \partial\Omega_F, \\ T \cdot N_C = C & \text{on} \quad \partial\Omega_C, \\ U = \lambda U_d & \text{on} \quad \partial\Omega_d, \end{cases} \tag{1}$$

where Ω is the occupied domain by the structure, T is the first Piola-Kirchhoff stress tensor, S is the second Piola-Kirchhoff stress tensor, B is the displacement gradient tensor, D is the fourth order elastic behavior tensor, γ is the Green-Lagrange strain tensor, λ is a control parameter, U_d, F and C are respectively an imposed displacement on the boundary $\partial\Omega_d$, an applied stress vector on the boundary $\partial\Omega_F$ and a stress vector of the unilateral contact on the boundary $\partial\Omega_C$, N_F and N_C are respectively the unit outward normal to the boundaries $\partial\Omega_F$ and $\partial\Omega_C$.

The problem can be rewritten in the following form:

$$\begin{cases} [L]\{T\} = \{0\} & \text{on} \quad \Omega, \\ \{T\} = ([A] + [B])\{S\}, & \\ \{S\} = [D]\{\gamma\}, & \\ [N_F]\{T\} = \lambda\{F\} & \text{on} \quad \partial\Omega_F, \\ \{U\} = \lambda\{U_d\} & \text{on} \quad \partial\Omega_d, \\ [N_C]\{T\} = \{C\} & \text{on} \quad \partial\Omega_C, \end{cases} \tag{2}$$

where $[L]$ is an operator matrix, $\{T\}$ and $\{S\}$ are vectors containing all the components of the first Piola-Kirchhoff stress tensor T and the second Piola–Kirchhoff stress tensor S, $[A]$ and $[B]$ are the matrices, $[N_F]$ and $[N_C]$ are matrices formed of components of the outward unit normal vectors to the boundary $\partial\Omega_F$ and $\partial\Omega_C$ respectively. We apply the perturbation technique as shown in [6] and using the definition of the path parameter [30], we obtain some linear problems given by:

$$\begin{cases} [L]\{T_k\} = \{0\} & \text{on} \quad \Omega, \\ \{T_k\} = [B_T]\{S_k\} + \left\{T_k^{nl}\right\}, & \\ \{S_k\} = [D_T]\{\gamma_k\} + \left\{S_k^{nl}\right\}, & \\ \{\gamma_k\} = [C_T]\{U_k^e\} + \left\{\gamma_k^{nl}\right\}, & \\ [N_F]\{T_k\} = \lambda_k\{F\} & \text{on} \quad \partial\Omega_F, \\ \{U_k\} = \lambda_k\{U_d\} & \text{on} \quad \partial\Omega_d, \\ [N_C]\{T_k\} = \{C_k\} & \text{on} \quad \partial\Omega_C, \end{cases} \tag{3}$$

where $(\cdot)^{nl}$ represent the terms that depend on solutions at previous orders and the matrices $[B_T]$, $[D_T]$ and $[C_T]$ are dependent on the initial solution.

Taking into account the MLS approximation of unknown vector $\{U\}$ and after substitution and assembly techniques, the problem of Eq. (3) can be written in the following condensed form:

$$\begin{cases} \text{Order:} \quad k = 1 & [K_T]\{U_1\} = \lambda_1\{F\} + \left\{F_1^{nl}\right\}, \\ \text{Order:} \quad 2 \leqslant k \leqslant p & [K_T]\{U_k\} = \lambda_k\{F\} + \left\{F_k^{nl}\right\}, \end{cases} \tag{4}$$

where $[K_T]$ is the stiffness matrix evaluated at a point solution, $\{F_k^{nl}\}$ is the term depending on previous orders solutions and $\{U_k\}$ is the unknown vector that collects all nodal displacements. The range of validity a_{max} of series expansion, in the path-following technique, is determinate by difference between consecutive orders. Simply, we require that the difference between two approximations to consecutive orders be quite small, which allows us to obtain an explicit formula $a_{max} = \left(\eta \frac{\|U_1\|}{\|U_p\|}\right)^{\frac{1}{p-1}}$, where η is a given tolerance parameter and $\|\cdot\|$ represents a given norm [30].

3. Optimum support size in high order meshfree approaches

Genetic algorithms are part of evolutionary algorithms which are based on genetics and natural selection. Their operation is extremely simple. We start from an initial population of arbitrarily chosen potential solutions (chromosomes). We assess their relative performance (fitness). These performances allow us to create another population of potential solutions by crossover, mutations, and selection which are simple evolutionary operators. This cycle must be repeated to find a satisfactory solution. The directed stochastic search makes genetic algorithms [31] a very robust and universal tool for almost any optimization problem which can be expressed in a reasonably small set of parameters.

The purpose is to use a search algorithm using the genetic algorithm to determine good size of influence domain h_i in the mesh-free methods. In this study, the genetic algorithm is tested to determine the good h_i for the simulation of large deformation problems. For a given distribution of points, this proposed strategy allows to determinate automatically and quickly the best number of neighbors points, to build the shapes functions, with good precision. We consider that the size of the influence domain $h_i = \beta ds$ where β is a coefficient to determinate and ds is the average distance between points, where

$ds = \frac{1}{N}\sum_{j=1}^{N} d_j$ and d_j is the distance between the jth point and its nearest natural neighbor. The proposed genetic algorithm for the optimal value search of the coefficient β is presented in Fig. 1. The idea is to minimize the relative error of the displacement at order 1 of the high order mesh-free algorithm [29, 32] as shown in this figure. This first order error estimator allows us to ensure a well-conditioned tangent matrix $[K_T]$ of the high order algorithm which is the same used in the other orders $k \geqslant 2$. For this reason, in the minimization of the relative error, we are limited to the displacement at order 1 to determine β_{optimal}.

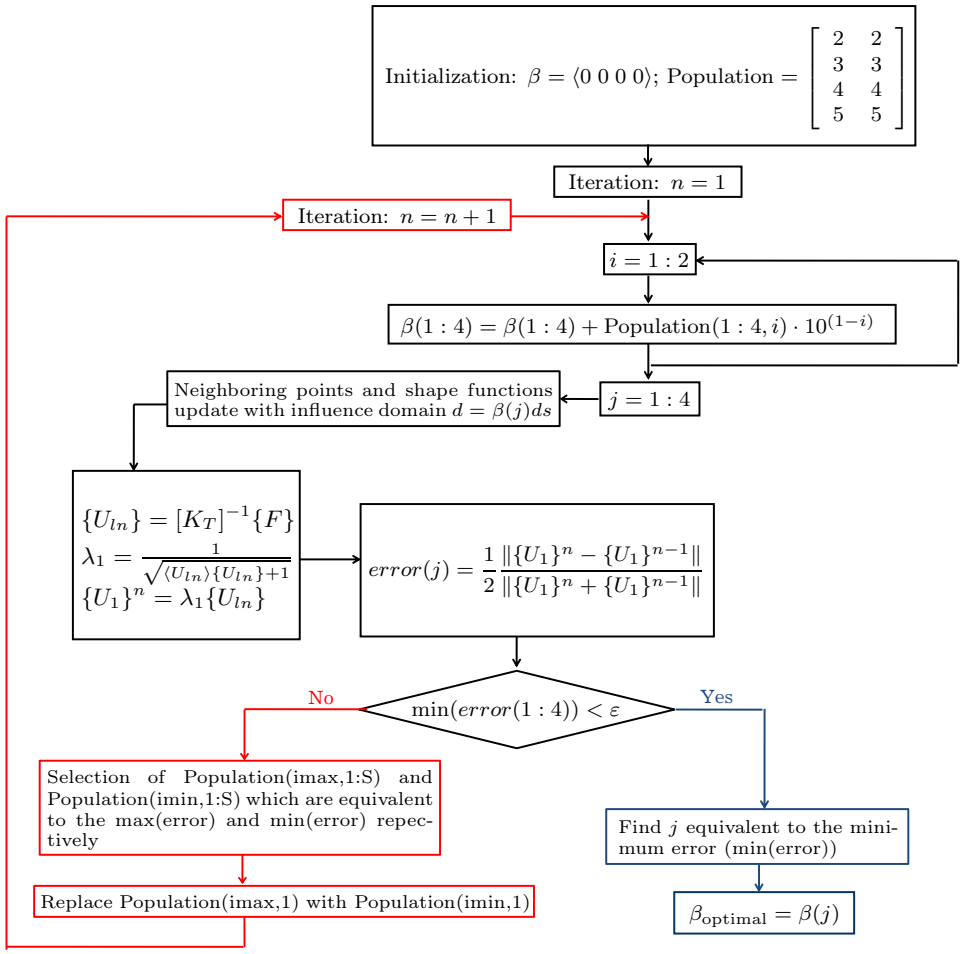

Fig. 1. Strategy of the genetic algorithm for finding the optimal value of β based on the first order error estimator.

In general, we can obtain the generation of the "Population" as follows:

$$\begin{aligned} \text{Population} &= \text{zeros}(N_{\text{population}}, \text{digits} + 1), \\ \text{Population} &= [\text{randi}([0\ 9], [N_{\text{population}}\ 1]), \ldots, \\ &\quad \text{randi}([0\ 9], [N_{\text{population}}\ \text{digits}])], \end{aligned} \tag{5}$$

where "$N_{\text{population}}$" represents the number of values β to be tested for each iteration, "digits" is the number of digits after the decimal point and "randi" is a random function between 0 and 9 where the size of the influence domain h_i varies in the interval $[0, 10]$. From our numerical experience on the use of the meshless strong form method for structural analysis and to facilitate understanding of the proposed algorithm, we limit the choices of the parameters of the genetic algorithm. In this contest, we can consider that the size of the influence domain h_i varies in the interval $[2, 5.5]$ as shown in the initial "Population" in the Fig. 1. We also assume a single number after the decimal point which limited to 2,

3, 4 and 5 as shown in the second column of "Population" (Population(:, 2)) of the initial "Population" where in this case β_{optimal} must be equal to 2.2, 3.3, 4.4 or 5.5. Note that in the selected "Population", the numbers in the first column of "Population" (Population(:, 1)) are arranged in ascending order from the smallest to the largest number to minimize the number of iterations in the proposed algorithm and to choose the smallest value of β_{optimal} with good precision to minimize the calculated time. The satisfactory solution is controlled by the displacement relative error which must be lower than of ε. If the relative errors of the values 2.2, 3.3, 4.4 and 5.5 are greater of the tolerance parameter ε, we change the values to be tested (Population(:, 1)) using the proposed strategy and keeping the same numbers after the commas (Population(:, 2)). We test the values of the new "Population" in the second iteration. The same procedure is repeated until the relative error is less than ε.

4. Numerical results

4.1. First example: the Timoshenko beam

Firstly, to guarantee the accuracy of the proposed approach, the relative error between the simulation results and the analytical solution is presented in the context of linear elasticity. We consider the Timoshenko beam [33] of the following mechanical properties: Young's modulus $E = 3 \cdot 10^7$ MPa, Poisson's ratio $nu = 0.3$. The geometrical properties of this beam are: length $L = 48$ mm, width $D = 12$ mm. The beam is considered to be of unit depth and is in a plane stress state (see Fig. 2).

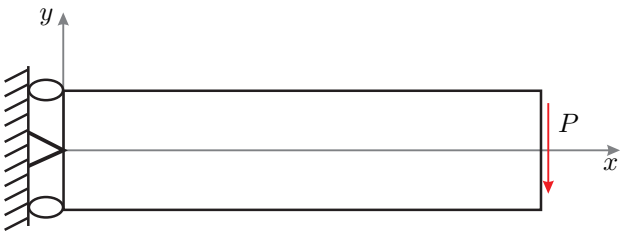

Fig. 2. The Timoshenko beam.

The beam is subjected to a parabolic traction, on the boundary at $(y, x = L)$, given by

$$F^d = \frac{-P}{2I}\left(\frac{D^2}{4} - y^2\right), \tag{6}$$

where $P = 1000$ and $I = \frac{D^3}{12}$ is the moment of inertia (second moment of the area). The exact displacement solution for this problem is

$$\begin{cases} u(x,y) = \dfrac{Py}{6EI}\left[(6Lx - 3x^2) + (2+\nu)\left(y^2 - \dfrac{D^2}{4}\right)\right], \\ v(x,y) = \dfrac{-Py}{6EI}\left[3\nu^2 y(L-x) + (4+5\nu)\dfrac{D^2 x}{4} + 3Lx - x^3\right]. \end{cases} \tag{7}$$

The satisfactory solution compared to the analytical solution is controlled by the displacement relative error $\frac{\|U_{\text{numerical}} - U_{\text{exact}}\|}{\|U_{\text{exact}}\|}$ which must be lower of $\varepsilon = 5 \cdot 10^{-3}$. The relative error of nodes displacements is computed according to the exact displacement solution in the equivalent positions of nodes. Fig. 3 shows the variation of the relative error of the nodes displacement with the parameter β using the genetic algorithm. The optimum value $\beta_{\text{optimal}} = 4.4$ can be obtained with a relative error equal to $6.858 \cdot 10^{-3}$ in the first iteration as shown the Fig. 3*a*. The first step in the second iteration is to create another population of potential solutions. In this work, we change the values to be tested (Population(:, 1)) using the proposed strategy and keeping the same numbers after the commas (Population(:, 2)). Therefore without taking into account the numbers after the decimal point, the value 5 equivalent to the maximum error is replaced by the value 4 equivalent to the minimum error and the new "Population" becomes:

$$\text{Population} = \begin{bmatrix} 2 & 2 \\ 3 & 3 \\ 4 & 4 \\ 4 & 5 \end{bmatrix}. \tag{8}$$

The first iteration allows to determine the best value of support size, but it is necessary to test other numbers after the decimal point to increase accuracy. Fig. 3*b* shows the second iteration where the optimum value $\beta_{\text{optimal}} = 4.5$ can be obtained with a relative error equal to $2.276 \cdot 10^{-3}$. The calculation stops because the relative error is lower of $\varepsilon = 5 \cdot 10^{-3}$ and the best choice of the optimal value is $\beta_{\text{optimal}} = 4.5$.

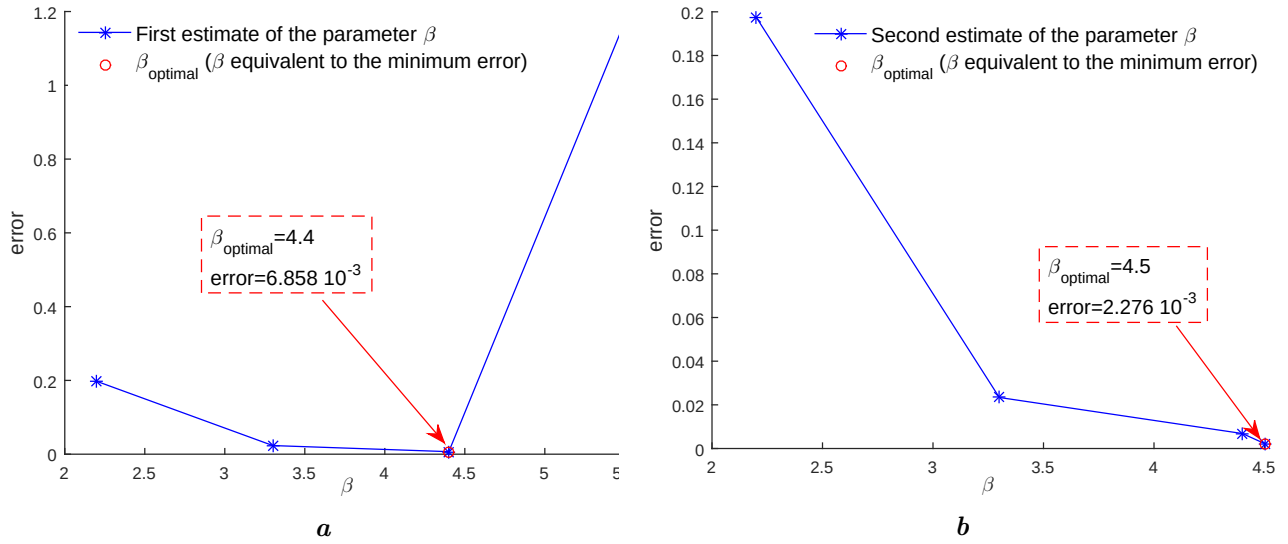

a ***b***

Fig. 3. Evolution of displacement relative error versus the parameter β: (***a***) First estimation of β_{optimal}; (***b***) Second estimation of β_{optimal}.

Fig. 4 represents the comparison of the analytical solution and that numerical of the adaptive algorithm based on meshless strong form approximation. To evaluate the obtained results, we compare in Table 1 the relative error $\frac{\|U-U_{exact}\|}{\|U_{exact}\|}$ of displacements calculated by the adaptive algorithm in bold and different values of support size. We observe an excellent agreement between the numerical and analytical result for the support size $hi = 4.5\,ds$ which can be determined automatically using our strategy based on the genetic algorithm. Otherwise, it should be noted that the arbitrary choice of support size requires many numerical tests to arrive at the same quality of the proposed strategy. This is what can make this strategy less expensive compared to the classical method. We can

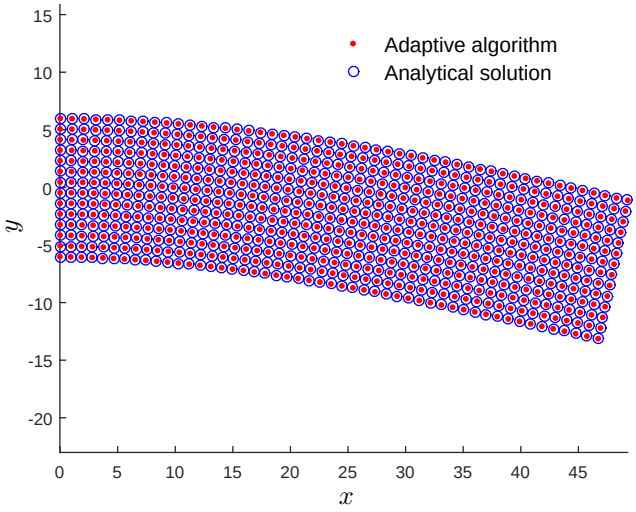

Fig. 4. Deformed configuration with deformation scale factor equal 800 for the adaptive algorithm and the analytical solution.

Table 1. Relative error $\frac{\|U_{\text{numerical}}-U_{\text{exact}}\|}{\|U_{\text{exact}}\|}$ using the proposed strategy and different values of the parameter β to approximate the shapes functions.

Parameter β	2	2.5	3	3.5	4	**proposed strategy**	5
Error (%)	31.573	1.748	2.012	2.521	2.2	**0.2276**	6.303

minimize the number of iterations by increasing the values tested in each iteration. For example, we consider that the number after the decimal point for each number 2, 3, 4 or 5 maybe 2, 3, 4 or 5 as shown in the initial population in Fig. 5. As shown the Fig. 6, the same quality solution can be obtained with a single iteration. In the following examples, we use the second choice of initial Population given

in Fig. 5 and the satisfactory solution is controlled by the displacement relative error (see Fig. 1) which must be lower of $\varepsilon = 10^{-4}$.

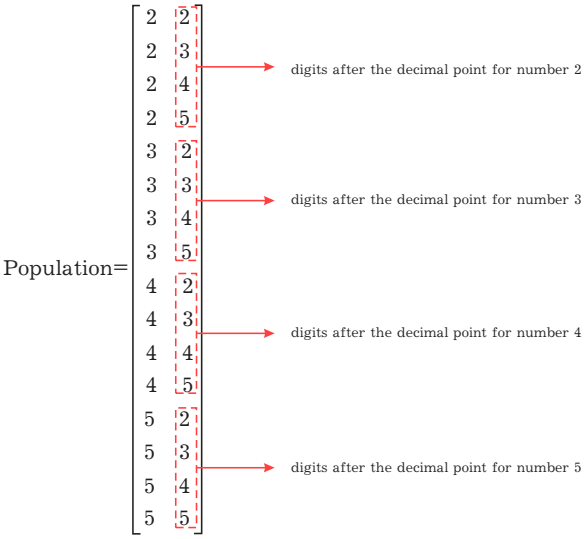

Fig. 5. Initial Population with the number after the decimal point for each number 2, 3, 4 or 5 maybe 2, 3, 4 or 5.

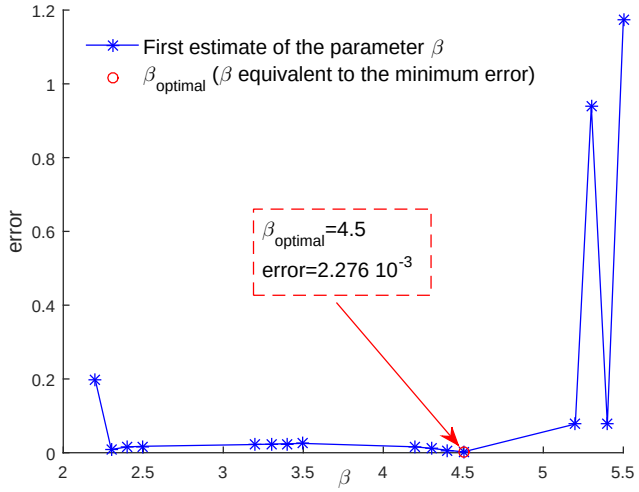

Fig. 6. Evolution of displacement relative error versus the parameter β.

4.2. Second example: traction of a bi-dimensional nonlinear elastic plate

Secondly, in the context of the geometrical non-linearity, we consider a bi-dimensional $2D$ elastic structure in tension of geometry (200 mm × 100 mm). This plate is fixed and submitted to a uniform loading λF ($F = 1$ MPa) at $x = 0$ and $x = L$ respectively. The mechanical properties of this structure are: Young's modulus $E = 2 \cdot 10^5$ MPa, Poisson's ratio $\nu = 0.3$.

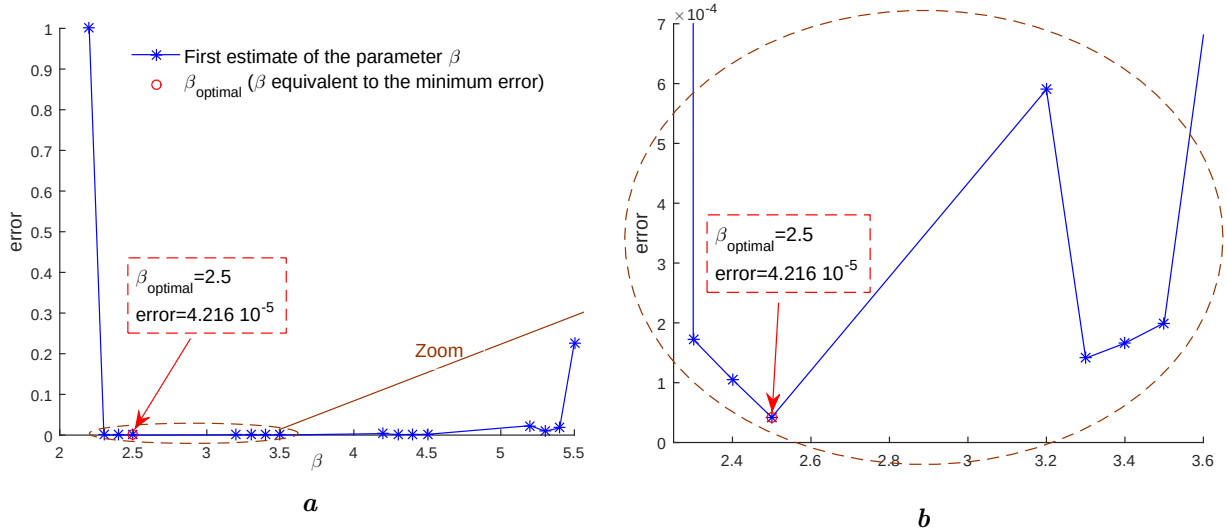

a ***b***

Fig. 7. Estimation of the optimal parameter β_{optimal}: (***a***) Evolution of displacement relative error versus the parameter β; (***b***) Zoom of the curve in the figure on the left.

In the numerical results, the proposed adaptive algorithm based on the high order mesh-free approach is denoted by "HOA-Adaptive". On the other hand, the high order approach using Finite Element Method FEM, considered as a reference solution, is denoted by "HOA-FEM". The chosen parameters of all high order mesh-free approaches ("HOA-Adaptive" and "HOA-FEM") are truncation order $p = 15$ and tolerance parameter $\eta = 10^{-8}$.

Fig. 7 shows the evolution of the displacement relative error with respect to the parameter β to estimate β_{optimal} in the first step using the genetic algorithm. The optimum value $\beta_{\text{optimal}} = 2.5$ can be obtained with a relative error equal to $4.216 \cdot 10^{-5}$.

Fig. 8 shows that the evolution of the optimal parameter β_{optimal} remains constant versus the number of steps, which explains that β_{optimal} is not influenced by the increase in loading and displacement. So in traction tests, we can search β_{optimal} just in the first step. In Fig. 9, we present the initial and the deformed configurations of the structure and the stress distributions S_{xx} in the plate for the load $\lambda = 2.2202 \cdot 10^5$.

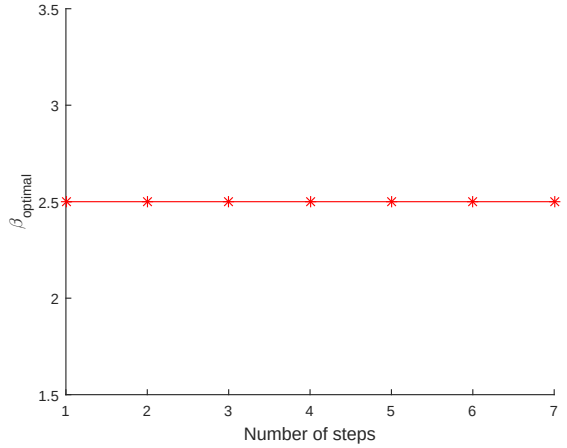

Fig. 8. Evolution of the optimal parameter β_{optimal} with respect to the number of steps using the "HOA-Adaptive".

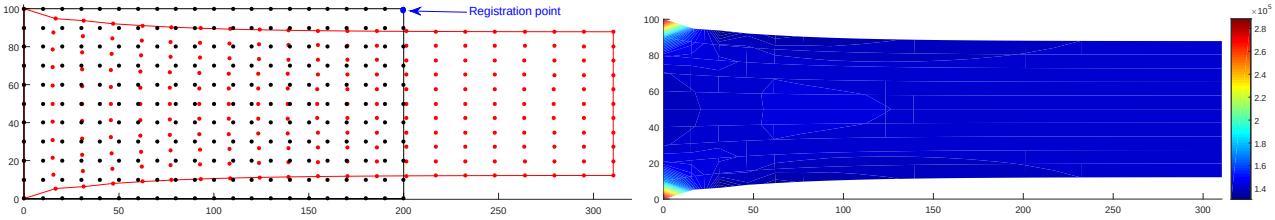

a ***b***

Fig. 9. Results for $\lambda = 2.2202 \cdot 10^5$: (***a***) Initial and deformed configurations of plate; (***b***) Distribution of stress component S_{xx} in the deformed configuration of plate.

We plot in Fig. 10 the evolution of the displacement components u and v with respect to the load parameter λ at registration point using the two algorithms "HOA-Adaptive" and "HOA-FEM". There is a good agreement between the two results where the maximum relative error of "HOA-Adaptive" versus "HOA-FEM" is less than 10^{-3}.

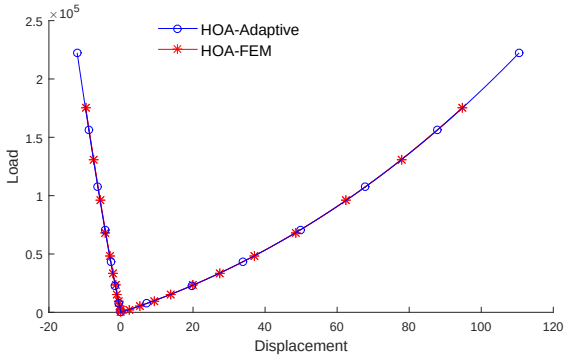

Fig. 10. Evolution of load λF with respect to displacements u and v for the two algorithms "HOA-Adaptive" and "HOA-FEM" at registration point.

4.3. Third example: bending of a bi-dimensional nonlinear elastic plate

In this third example, we consider the bending of a bi-dimensional $2D$ elastic structure of geometry (200 mm × 20 mm) with the same mechanical properties and the same chosen parameters of the first example for the algorithm "HOA-Adaptive". This plate is fixed at $x = 0$ and submitted to an imposed bending load λF ($F = 1$ MPa) at $x = L$.

Using the genetic algorithm, Fig. 11*a* shows the evolution of displacement relative error with respect to the parameter β to estimate β_{optimal} in the first step. The optimum value $\beta_{\text{optimal}} = 3.4$ can be obtained with a relative error equal to $2.146 \cdot 10^{-5}$ which represents the minimum value as shown the Fig. 11*b*.

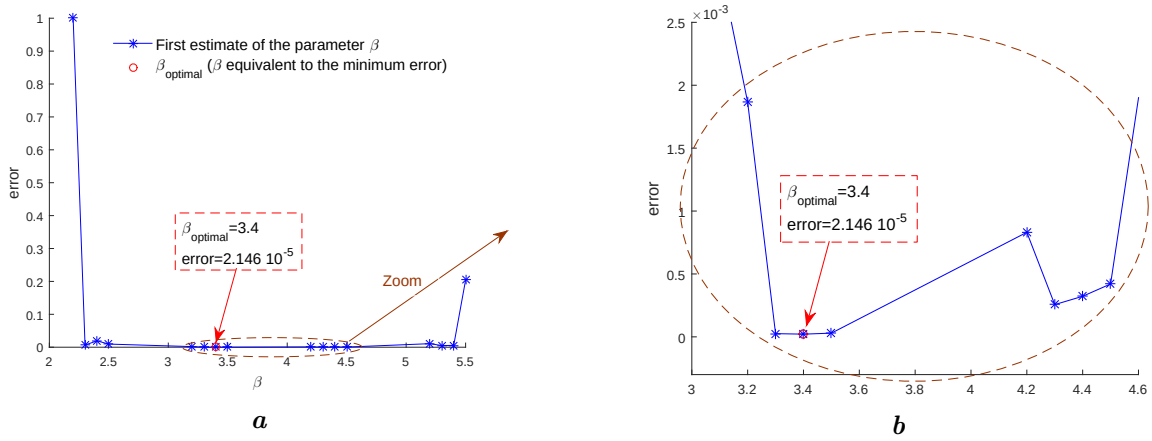

Fig. 11. Estimation of the optimal parameter β_{optimal}: (***a***) Evolution of displacement relative error versus the parameter β; (***b***) Zoom of the curve in the figure on the left configuration of plate.

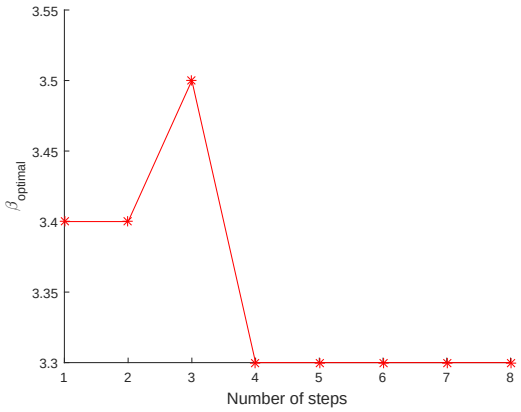

Fig. 12. Evolution of the optimal parameter β_{optimal} with respect to the number of steps using the "HOA-Adaptive".

In the bending test, the optimal parameter β_{optimal} varies between 3.3 and 3.5 (see Fig. 12). Initial and deformed configurations of the plate and the distribution of the stress component S_{xx} in the deformed configuration of the plate for $\lambda = 4569$, in the case of the bending test, are represented in the Fig. 13.

We also represent in Fig. 14, the evolution of load λF with respect to displacements u and v for the two algorithms "HOA-Adaptive" and "HOA-FEM" at the registration point. The results show that the maximum relative error of "HOA-Adaptive" versus "HOA-FEM" is less than 10^{-3}, but the convergence radius of "HOA-FEM" tends to zero and the calculation stops from the load value $\lambda = 3500$. But "HOA-Adaptive" exceeds this value, which shows the advantage of the high order mesh-free approach compared to high order approach based on the FEM.

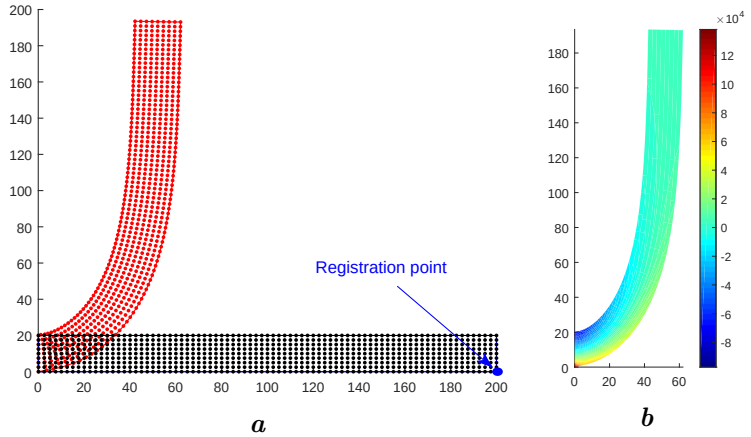

Fig. 13. Results for $\lambda = 4569$: (***a***) Initial and deformed configurations of plate; (***b***) Distribution of stress component S_{xx} in the deformed configuration of plate.

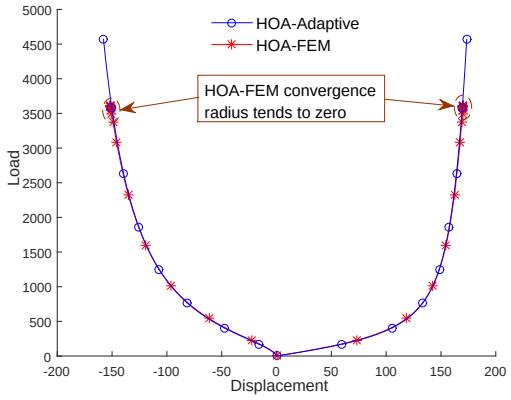

Fig. 14. Evolution of load λF with respect to displacements u and v for the two algorithms "HOA-Adaptive" and "HOA-FEM" at the registration point.

4.4. Fourth example: bending of a bi-dimensional nonlinear elastic plate in contact with a rigid foundation

In this test, the contact between the bi-dimensional nonlinear elastic structure and a rigid foundation is considered as shown in the initial configuration of the plate in Fig. 15*a*. We adopt the same mechanical and geometrical data as in the second example. We are interested to treat this problem by using the proposed algorithm "HOA-Adaptive" based on a genetic algorithm. Fig. 15 represents the deformed configuration of the plate (see Fig. 15*a*) for the load parameter $\lambda = 48.3963$ and distribution of the stress component S_{xx} in the deformed plate (see Fig. 15*b*) for the same load parameter.

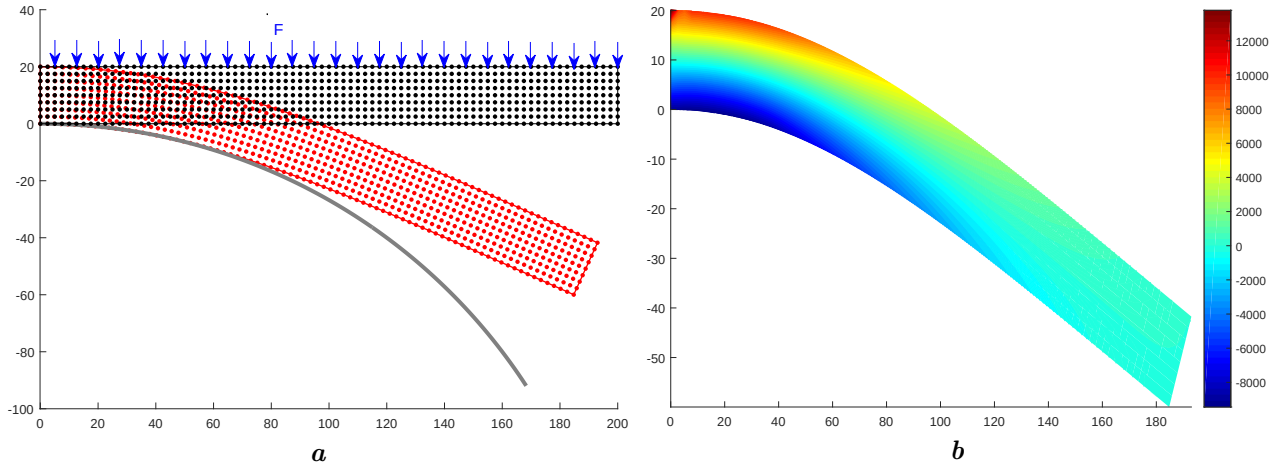

Fig. 15. Results for $\lambda = 48.3963$: (***a***) Initial and deformed configurations of the plate; (***b***) Distribution of the stress component S_{xx}.

Fig. 16 illustrates the evolution of displacement relative error versus the parameter β in the first step ($k = 1$). The analysis of this figure shows that the optimal value is $\beta_{\text{optimal}} = 3.3$ with a relative error equal to $2.09 \cdot 10^{-5}$.

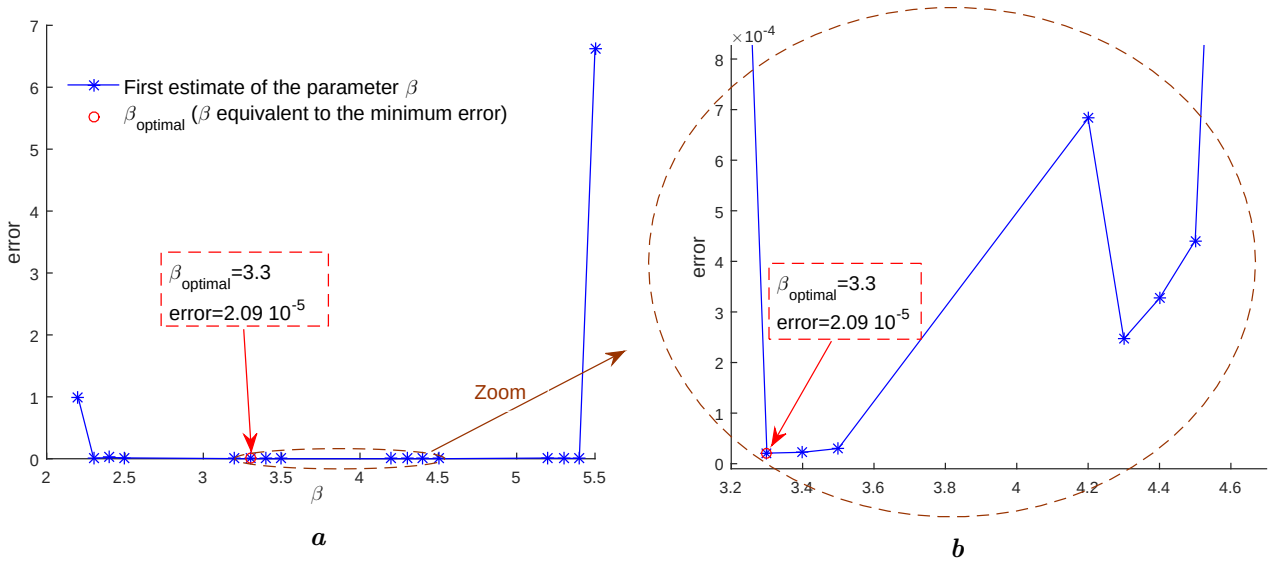

Fig. 16. Estimation of the optimal parameter β_{optimal}: (***a***) Evolution of displacement relative error versus the parameter β; (***b***) Zoom of the curve in the figure on the left.

Fig. 17 shows the evolution of the optimal parameter β_{optimal} with respect to the number of steps. We remark that there is a fluctuation of β_{optimal}, which the optimal parameter β_{optimal} varies of 3.3 to 3.5, after that the calculation stabilizes.

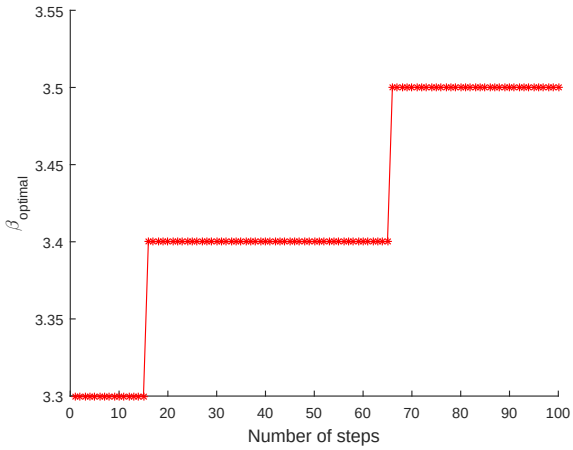

Fig. 17. Evolution of the optimal parameter β_{optimal} with respect to the number of steps using the "HOA-Adaptive".

5. Conclusion

In this paper, we present a new strategy for the automatic adaptation of the support size of meshfree approaches. In this strategy, we have adapted an algorithm for finding the optimal value of support size with a high order meshfree algorithm. The proposed adaptive mesh-free approach based on this strategy gives good results with good precision, compared with the high order approach based on FEM, which overcomes the difficulty for finding the size of influence domain. This work is an initiation in this field who can handle some technical difficulties in meshless methods and to show the effectiveness of the new strategy for finding the optimal value of the support size, therefore the proposed strategy allows us to think about implementing mesh-free approaches in industrial simulation software.

[1] Chen J. S., Pan C., Wu C. T., Liu W. K. Reproducing kernel particle methods for large deformation analysis of non linear structures. Computer Methods in Applied Mechanics and Engineering. **139**, 195–227 (1996).

[2] Kargarnovin M. H., Toussi H. E., Fariborz S. J. Elasto-plastic element-free galerkin method. Computational Mechanics. **33**, 206–214 (2004).

[3] Belinha J., Dinis L. M. Elastoplastic analysis of plates by the element free Galerkin method. International Journal of Computer Aided Engineering and Software. **23**, 525–551 (2006).

[4] Belinha J., Dinis L. M. Nonlinear analysis of plates and laminates using the element free Galerkin method. Composite Structures. **78**, 337–350 (2007).

[5] Chen S. S., Liu Y. H., Cen Z. Z. Lower bound shakedown analysis by using the element free Galerkin method and non linear programming. Computer Methods in Applied Mechanics and Engineering. **197**, 3911–3921 (2008).

[6] Belaasilia Y, Timesli A, Braikat B., Jamal M. A numerical mesh-free model for elasto-plastic contact problems. Engineering Analysis with Boundary Elements. **82**, 68–78 (2017).

[7] Alfaro I., Racineux G., Poitou A., Cueto E., Chinesta F. Numerical Simulation of Friction Stir Welding by Natural Element Methods. International Journal of Material Forming. **1**, 1079–1082 (2008).

[8] Timesli A., Braikat B., Lahmam H., Zahrouni H. An implicit algorithm based on continuous moving least square to simulate material mixing in friction stir welding process. Modelling and Simulation in Engineering. **2013**, 1–14 (2013).

[9] Timesli A., Braikat B., Lahmam H., Zahrouni H. A new algorithm based on Moving Least Square method to simulate material mixing in friction stir welding. Engineering Analysis with Boundary Elements. **50**, 372–380 (2015).

[10] Mesmoudi S., Timesli A., Braikat B., Lahmam H., Zahrouni H. A 2D mechanical-thermal coupled model to simulate material mixing observed in Friction Stir Welding process. Engineering with Computers. **33**, 885–895 (2017).

[11] Rao B. N., Rahman S. An enriched meshless method for non-linear fracture mechanics. International Journal for Numerical Methods in Engineering. **59**, 197–223 (2004).

[12] Xu Y., Saigal S. Element free Galerkin study of steady quasi-static crack growth in plane strain tension in elastic-plastic materials. Computational Mechanics. **22**, 255–265 (1998).

[13] Xu Y., Saigal S. An element-free galerkin analysis of steady dynamic growth of a mode i crack in elastic-plastic materials. International Journal of Solids and Structures. **36**, 1045–1079 (1999).

[14] Liu T., Liu G., Wang Q. An element-free Galerkin-finite element coupling method for elasto-plastic contact problems. Journal of Tribology. **128**, 1–9 (2005).

[15] Rabczuk T., Areias P., Belytschko T. A meshfree thin shell method for nonlinear dynamic fracture. International Journal for Numerical Methods in Engineering. **72**, 524–548 (2007).

[16] Alfaro I., Yvonnet J., Cueto E., Chinesta F., Doblaré M. Meshless Methods with Application to Metal Forming. Computer Methods in Applied Mechanics and Engineering. **195**, 6661–6675 (2006).

[17] Li S., Hao W., Liu W. K. Mesh-free simulations of shear banding in large deformation. International Journal of solids and structures. **37**, 7183–7206 (2000).

[18] Martinez M. A., Cueto E., Alfaro I., Doblaré M., Chinesta F. Updated lagrangian free surface flow simulations with Natural Neighbour Galerkin methods. International Journal for Numerical Methods in Engineering. **60**, 2105–2129 (2004).

[19] Li S., Liu W. K. Reproducing kernel hierarchical partition of unity part I: formulation and theory. International Journal for Numerical Methods in Engineering. **45**, 1285–1309 (1999).

[20] Li S., Liu W. K., Rosakis A., Belytschko T., Hao W. Mesh-free Galerkin simulations of dynamic shear band propagation and failure mode transition. International Journal of solids and structures. **39**, 1213–1240 (2002).

[21] Liu W. K., Junn S., Li S., Adee J. Reproducing Kernel Particle Methods for structural dynamics. International Journal for Numerical Methods in Engineering. **38**, 1655–1679 (1995).

[22] Liu W. K., Jun S., Zhang Y. F. Reproducing Kernel Particle Methods. International Journal for Numerical Methods Fluids. **21**, 1081–1106 (1995).

[23] Liu W. K., Li S., Belytschko T. Moving least square reproducing kernel method (I) methodology and convergence. Computer Methods in Applied Mechanics and Engineering. **143**, 113–154 (1997).

[24] Dolbow J., Belytschko T. Volumetric locking in the finite element free Galerkin method. International Journal for Numerical Methods in Engineering. **46**, 925–942 (1999).

[25] De S., Bathe K. J. Displacement/pressure mixed interpolation in the method of finite spheres. International Journal for Numerical Methodsin Engineering. **51**, 275–292 (2001).

[26] Liu W. K., Chen Y., Jun S., Chen J. S., Belytschko T. Advances in multiple scale kernel particle methods. Computational Mechanics. **18**, 73–111 (1996).

[27] El Kadmiri R., Belaasilia Y., Timesli A., Kadiri M. S. A coupled Meshless-FEM method based on strong-form of Radial Point Interpolation Method (RPIM). Journal of Physics: Conference Series. **1743**, 012039 (2021).

[28] El Kadmiri R., Belaasilia Y., Timesli A., Kadiri M. S. Meshless approach based on MLS with additional constraints for large deformation analysis. Journal of Physics: Conference Series. **1743**, 012015 (2021).

[29] Timesli A. Optimized radius of influence domain in meshless approach for modeling of large deformation problems. Iranian Journal of Science and Technology-Transactions of Mechanical Engineering. (2021).

[30] Cochelin B. A path-following technique via an asymptotic-numerical method. Computer and Structures. **53**, 1181–1192 (1994).

[31] Mitchell M. An Introduction to Genetic Algorithms. Cambridge, MA, MIT Press (1996).

[32] Saffah Z., Timesli A., Lahmam H., Azouani A., Amdi M. New collocation path-following approach for the optimal shape parameter using Kernel method. SN Applied Sciences. **3**, 249 (2021).

[33] Dolbow J., Belytschko T. An introduction to programming the meshless element free Galerkin method. Archives of Computational Methods in Engineering. **5**, 207–241 (1998).

Оптимальна підтримка змінного розміру для безсіткових підходів з використанням генетичного алгоритму

Гассуна С., Таймслі А.

Університет Касабланки Хасан II,
Національна вища школа мистецтв та ремесел (Ensam Casablanca),
20670 Касабланка, Марокко

Основна складність безсіткових методів пов'язана з підтримкою форми функцій. Ці методи стають стабільними, коли використовується достатньо велика підтримка. Значно більший розмір підтримки призводить до більших обчислень та значно гіршої якості. Неперервне регулювання розміру підтримки для апроксимації функцій форми під час моделювання може усунути цю проблему, але вибір розміру підтримки відносно локальної щільності не є простою проблемою. У даній роботі досліджується розумний розмір домену впливу, використовуючи генетичний алгоритм у поєднанні з безсітковими алгоритмами високого порядку, оптимальне значення яких залежить від точності та стабільності результатів. Пропонована стратегія забезпечує гарантії щодо зростання похибок наближення, контроль рівня похибки, а також адаптацію стратегії оцінки для досягнення необхідного рівня точності. Це дозволяє адаптувати запропонований алгоритм до необхідної складності задачі. Запропонована стратегія у безсіткових підходах випробовується на деяких прикладах структурного аналізу.

Ключові слова: *великі деформації, сильна форма, безсітковий метод, генетичний алгоритм, автоматичний вибір найближчого околу.*